IMPROVED IDQC RECONSTRUCTION FOR INHOMOGENEITY CORRECTED MR SPECTROSCOPY

Rohini Shankar[1]*, Tianliang Gu*[2]*, Jianhui Zhong*[2]*, Mathews Jacob*[2,3]

[1]Dept. of ECE, [2]Dept. of Imaging Sciences, [3]Dept. of Biomedical Engineering
University of Rochester

ABSTRACT

In this paper, we focus on the reconstruction of iDQC MR spectroscopy data. Unlike standard 1-D MR spectroscopy schemes, iDQC acquires 2-D spectral data to decouple the magnetic field inhomogeneity effects from chemical shift information. This method suffers from a few limitations such as low intrinsic SNR, long acquisition time and the presence of a strong residual water peak. The standard IFFT based reconstruction scheme that rely on uniform sampling patterns have limited ability to overcome these problems. We propose a novel reconstruction scheme that employs a non-uniform sampling pattern, based on a flexible partitioning of the 2-D data-space. This approach enables the reconstruction of the metabolite region with a good resolution and signal to noise ratio, without being affected by aliases from the residual water signals. We pose the reconstruction problem as a conjugate gradient optimization. Using phantom data, we illustrate the significantly improved performance of the new method.

Index Terms— MRS, iDQC, sampling, Reconstruction

1. INTRODUCTION

In recent years, magnetic resonance spectroscopy (MRS) is being increasingly used for the estimation of in-vivo metabolite concentrations, mainly within the brain. It is shown that the variations of metabolite concentrations, measured with MRS, is indicative of various abnormalities such as cancer, neuro-AIDS and Alzheimer's disease.

The inhomogeneity of the main magnetic field is an important challenge that limits the applicability of MRS to in-vivo applications. Standard quantification algorithms model the line-shape distortion as a simple convolution [1]; the spectral data is assumed to be convolved with a parametrically represented point-spread function (PSF). The PSF is estimated from the MRS data itself. However, the point-spread function is dependent on the spatial variations of the metabolites as well as the spatially varying field-map. Hence, each metabolite will have its own PSF, as opposed to a common PSF assumed by the LCModel. This assumption of the common PSF breaks down for large voxels; this limits the ability of standard quantification schemes for the estimation of metabolite concentrations from large sub-regions of the brain, say the cerebellum.

To overcome these problems, a novel two-dimensional MRS scheme called as intermolecular Double Quantum Coherences (iDQC) was recently introduced [2, 3]. In contrast to the one-dimensional acquisition scheme in standard MRS, the iDQC scheme acquires 2-D spectral data. In addition to the standard chemical shift dimension (denoted by f_2, whose dual dimension is indicated by t_2), it acquires an extra dimension (denoted by f_1). The dual axis of f_1 is denoted by t_1. The iDQC scheme encodes the field-inhomogeneity information along the t_1 axis. This approach enables the decoupling of the field-inhomogeneity effects and chemical shift information, thus leading to field-inhomogeneity independent spectral estimation.

Despite the above mentioned advantages, the iDQC scheme suffers from a few drawbacks in the in-vivo setting. Since the signal is generated by double quantum effects, the intrinsic SNR is significantly lower than standard MRS schemes. Furthermore, as we increase t_1, the signal to noise ratio drops considerably due to increased T_2 decay. Since, the data is acquired without water suppression, huge nuisance peaks from the water signal are distributed on a large region of the $f_1 - f_2$ plane. To properly correct the field-inhomogeneity induced distortions, we require good resolution reconstructions along the f_1 axis. Broad point spread functions along this axis could introduce cross-talk between regions with different field-map values, thus leading to uncorrected line-shape distortions and line broadening. The standard iDQC scheme uses uniform sampling of the t_1 dimension. The 2-D iDQC signal is then reconstructed using the standard 2-D IFFT [3]. Although the metabolites are distributed over a narrow range of frequencies along the f_1 dimension, a large band-width (along f_1) is often required to avoid the aliases from the residual water signal. This implies that a large number of samples are required to obtain the reconstructions with reasonable resolution. Moreover, the SNR of the acquired samples decrease significantly due to T_2 decay as we increase t_1.

We propose a novel reconstruction scheme to overcome these problems. We partition the $f_1 - f_2$ plane into two regions, corresponding to metabolite and nuisance water signal

respectively. We will seek to reconstruct the metabolite region with good signal to noise ratio and resolution, while the nuisance signal region will be reconstructed at a lower resolution. To ensure this, we will use a non-uniform sampling pattern derived by combining two uniform patterns. The coarse pattern enables the high-resolution reconstruction of the metabolite region, while the dense pattern provides increased SNR for the metabolites. The dense pattern also enables the reconstruction of the residual water signal at a low resolution, thus preventing it aliasing to the metabolite regions. We pose the reconstruction problem as a conjugate gradients (CG) optimization scheme. Validations using phantom data indicate that the non-uniform pattern provides significantly improved results over the standard uniform pattern.

2. BACKGROUND

In contrast to the standard 1-D acquisition scheme, iDQC uses a 2-D method. The iDQC signal is generated by double quantum interactions between the strong water signal and the metabolites. Consider a system consisting of water (indicated by w) and a metabolite (indicated by m). In the absence of any field inhomogeneity, the iDQC signal from this system of two singlets is proportional to

$$f(\omega_1, \omega_2) \propto \rho \cdot \delta \left(\omega_1 - \omega_w, \omega_2 - \frac{\omega_m}{2} \right), \qquad (1)$$

where ρ is the concentration of the metabolite, ω_w is the frequency of water, and ω_m the frequency of the metabolite. Here δ denotes the 2-D Dirac delta function. In the context of in-vivo acquisitions, different spatial locations in the selected region will have different field strengths due to the inhomogeneity of the field. Hence, the water and metabolite signals at a specified location $\mathbf{x}$ will be precessing at $\omega_w + \Delta\omega(\mathbf{x})$ and $\omega_m + \Delta\omega(\mathbf{x})$ respectively, where $\Delta\omega(\mathbf{x}) = \gamma \Delta B(\mathbf{x})$, γ being the gyromagnetic ratio and $\Delta B(\mathbf{x})$ the variation in the field homogeneity. Thus, the iDQC signal from a specified location $\mathbf{x}$ is given by

$$f(\omega_1, \omega_2, \mathbf{x}) \propto \rho_{\mathbf{x}}(\Delta\omega)\, \delta \left(\omega_1 - \Delta\omega(\mathbf{x}), \omega_2 - \frac{\omega_m + \Delta\omega(\mathbf{x})}{2} \right) \qquad (2)$$

In the above equation, we have assumed the frequency of water to be zero: $\omega_w = 0$. In the presence of an inhomogeneous field, the net signal will be distributed along a line, centered at ω_m, with an angle of $26.6^\circ = \arctan(1/2)$ with respect to the f_2 axis. The amplitude of the signal at any specified location on the line will be indicative of the net concentration of the metabolite at corresponding $\Delta\omega$.

Figure(1) illustrates the intermolecular cross-peaks of Water, Creatine, Choline and NAA (N-Acetyl Aspartate) extended along the lines that make an angle of 26.6° with respect to the f_2 axis. Since all the field-induced variations are localized along these lines, the 1-D spectrum is obtained by evaluating the line-integral

$$g(\omega_2) = \int f(\omega, \omega_2 + \omega/2) d\omega. \qquad (3)$$

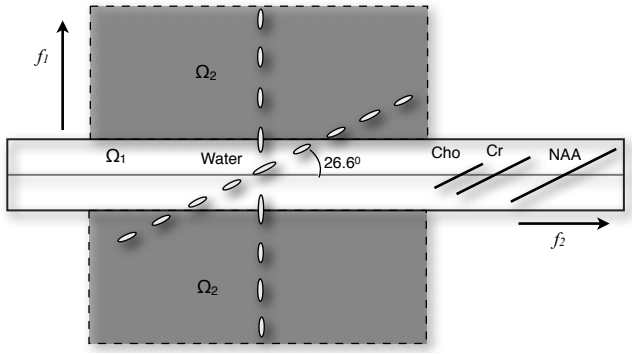

Fig. 1. Intermolecular cross-peaks of Cr, Cho and Naa at an angle of 26.6° to the f_2 axis. The f_1-f_2 plane is partitioned into regions Ω_1 and Ω_2 as illustrated. Ω_1 includes the metabolite streaks and Ω_2 spans the expanse of the residual water resonance. The central dotted line parallel to the f_1 axis as well as the dotted line oriented at 26.6° show the extent of the nuisance signal from water.

3. PROPOSED METHOD

The iDQC acquisition consists of a sequence of readouts, each corresponding to a different value of t_1. The entire line (all values of t_2 at the specified t_1 value) is acquired during the read-out. We use the standard residual water suppression technique, wherein a low pass filter is applied to each readout. As with any water suppression scheme, this method provides significantly reduced water peaks. However, significant residual water signal is often present along the f_1 and f_2 axis, as well as at the angle of 26.6° with respect to the f_2 axis (see Fig. 1). In contrast to the residual water signal that is distributed over a large region, the metabolite signals are localized to a very small band Ω_1 which spans only half the expected range of the field-map. Poor resolution of the reconstructions (along f_1) will lead to cross-talk between spectral regions and hence distort the resulting 1-D metabolite signals (see Fig 4-a & b) . Hence, we would like to reconstruct the signals in Ω_1 at a very good resolution.

The standard practice is to reconstruct the signal in a rectangular region (of width w) that covers both the water and metabolite regions. The voxel-size of the reconstruction along the f_1 axis is given by w/N, where N is the number of t_1 steps. Since w is large, many acquisitions (t_1 steps) are required to obtain a reasonable resolution; due to scan time limitations, one often settles for a low resolution. Moreover, the limited scan time will also restrict the number of averages that

can be acquired. In the next subsection, we propose a more flexible method that will enable us to improve the SNR of the reconstructions without increasing the distortion.

3.1. Choice of the reconstruction and sampling scheme

For a moment, let us assume that we only need to reconstruct the metabolite signals localized to Ω_1. The resolution along the f_1 axis is given by w_1/N_1, where N_1 is the number of acquisitions (t_1 steps). Since $w_1 << w$, the number of t_1 steps required to acheive the same resolution is $N_1 << N$. This implies that with this scheme, one can perform more averages in a given acquisition time. Since the sensitivity falls with increasing t_1, it is common practice in spectroscopy to acquire averages only for the lower samples . The reconstructions can be performed using an IFFT of the averaged data. Qualitatively similar results could can be obtained by using an iterative algorithm to reconstruct the signal on Ω_1, using the non-uniform acquisition scheme shown in Fig 2.b.

As discussed before, the water signal is distributed on a much larger region on the frequency plane. The reconstruction of the signals, assuming them to be only localized to Ω_1, will lead to strong aliasing artifacts from the water signal. To avoid these artifacts, we propose to reconstruct the signal in Ω_2 at a lower resolution. This approach ensures that the water signals do not alias to Ω_1, corrupting the metabolite signals. In addition to providing higher SNR for signals in Ω_1, the dense sampling of the lower t_1 space will enable the low-resolution reconstruction of the residual water signal in Ω_2. Specifically, this approach will significantly minimize the aliasing artifacts. We choose the sampling rates as $\Delta T_1 = 1/w_1$ and $\Delta T_2 = 1/w$.

3.2. Iterative reconstruction scheme

We pose the reconstruction problem as an optimization scheme, where the cost function is defined as

$$C(f) = ||b - Af||^2 + \lambda_1 ||\nabla f||^2_{\Omega_1} + \lambda_2 ||\nabla f||^2_{\Omega_2} \qquad (4)$$

The first term is the data consistency term that penalizes the discrepacy between the original measurements and the Fourier samples of the reconstructed signal. The second and third terms correspond to the norm of the gradients in Ω_1 and Ω_2 respectively. By choosing the values of λ_1 and λ_2 different, we control the resolution of the reconstructed signal in the corresponding regions. The final iDQC reconstruction is given by the minimization of Eq. (4) :

$$f^* = \arg\min_f C(f) \qquad (5)$$

We use conjugate gradients optimization scheme to solve for the optimal f. The gradient of this criterion at the n^{th} iteration is given by

$$\partial C(f_n) = \begin{cases} A^H(Af_n - b) + \lambda_1 \nabla^2 f_n & \text{in} \quad \Omega_1 \\ A^H(Af_n - b) + \lambda_2 \nabla^2 f_n & \text{in} \quad \Omega_2 \end{cases} \qquad (6)$$

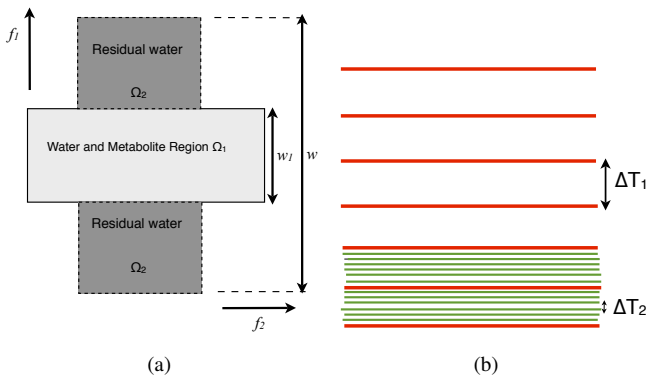

Fig. 2. (a) Flexible partitioning of the f_1-f_2 plane and (b) the non-uniform sampling scheme. The width of Ω_1 is denoted by w_1 and the width of composite region ($\Omega_1 \bigcup \Omega_2$) is denoted by w. We choose $\Delta T_1 = \frac{1}{w_1}$ and finer step-size $\Delta T_2 = 1/w$. Samples placed at a coarse step-size of ΔT_1 enable the reconstruction of the metabolite signal in Ω_1. The finer samples (spaced at ΔT_2) enable the reconstruction of signals in Ω_2 at a low resolution, preventing water from aliasing into the metabolite region. Moreover, they also aid in improving the SNR of the metabolites.

The Laplacian operator ∇^2 is discretized using second-order forward finite differences. The iterations are terminated when the ratio of the decrease in the cost criterion to the initial cost criterion falls below a specified threshold value.

4. RESULTS

A Siemens Trio 3T MRI system was used to acquire the 2D data for a phantom consisting of the metabolites Choline (Cho), Creatine, (Cr) and N-acetyl Aspartate (NAA) dissolved in water. The measurements were conducted for a voxel size of 3.5x3.5x3.5cm^3. Fig. (3)-a& b depicts the standard single voxel MRS over a 3.5x3.5x3.5 cm^3 voxel in the phantom at good and bad shimming respectively. The linewidth of the SVS data-sets were rougly 5 Hz and 20 Hz respectively. The rest of the experiments are focused on deriving intelligible spectrum from the poorly-shimmed region.

The iDQC data was collected on the same region and settings as used in Fig. 3.b. 1024 samples in the f_2 dimension and 256 samples in the f_1 dimension were acquired. Of the 256 samples, the first 32 samples were acquired using a step-size of 1 ms and the remaining 224 samples at a step-size of 4 ms. This data-set was later sub-sampled for the experiments.

Fig. 4-a&b indicates the standard IDQC reconstructions with $\Delta T_1 = 2$ms. An 250 point IFFT is used to reconstruct the 2-D data with a 500 Hz bandwidth along the f_1 dimension. The approximate resolution for the metabolite region Ω_1 is 4.3 Hz. Although the peaks are clearly visible, the poor resolution along f_2 (see Fig.4-a) has resulted in large linewidths. Also note from (a) that the patterns are not oriented

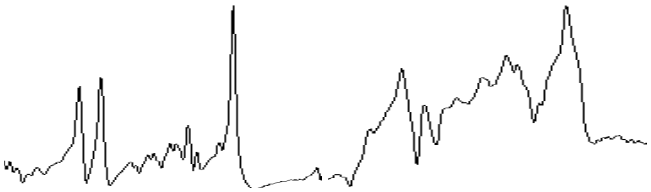

(a) (b)

Fig. 3. (a) and (b) Single voxel Spectroscopy: (a) Data set acquired from a brain phantom with good shimming. The linewidth is approximately 6 Hz in this case. Note that the NAA, Creatine and Choline peaks are well depicted. (b) Data set acquired from the same region with bad shimming. The linewidth is approximately $\pm$20 Hz. Note that none of the peaks can be resolved in this case.

along 26.6° as theoretically predicted in iDQC. This is due to the poor resolution along the f_1 axis; the peaks are blurred along the f_1 dimension.

Fig. 4-c&d uses a uniform spacing of $\Delta T_1 = 16$ms. A 62 point IFFT is used to reconstruct the 2-D data with a 62 Hz bandwidth along the f_1 dimension. The approximate resolution for the metabolite region Ω_1 is 1.06 Hz. Note that the NAA peak is visible and is The SNR is pretty bad in this case, resulting in poor reconstruction of the Creatine and Choline peaks.

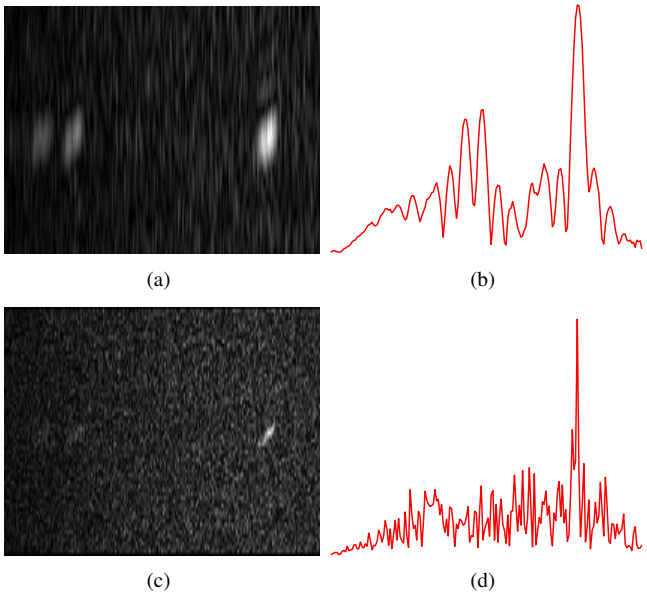

(a) (b)

(c) (d)

Fig. 4. Standard IFFT-based IDQC reconstructions using uniform sampling patterns. 58 t_1 steps were chosen in both cases. A spacing of $\Delta T_1 = 4$ms was chosen to reconstruct (a) and (b). The spacing $\Delta T_1 = 16$ms was used in (c) and (d).

Fig. 5 shows the reconstructions using the sampling pattern shown in Fig. 2. We have chosen ΔT_1=16ms and ΔT_2=1ms. 32 samples, spaced at 1ms were used in the lower region and the remaining 26 samples were spaced at 16ms each. The two regions Ω_1 and Ω_2 were set up such that $w_1 = 60$ and $w = 1000$. Clearly the non-uniform pattern performed better as all the three metabolite peaks are clearly resolved. In comparison, the uniform patterns, the non-uniform pattern provided a good compromise between resolution and SNR.

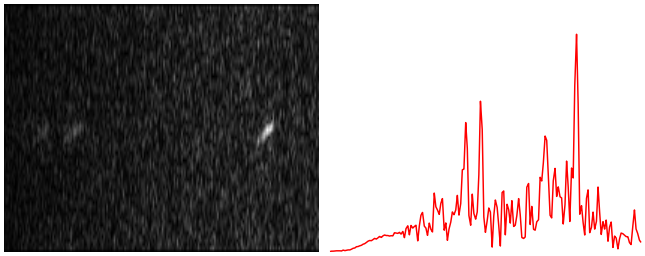

(a) (b)

Fig. 5. CG reconstructions utilizing 58 non-uniform samples at ΔT_1=16ms and ΔT_2=1ms; the sampling scheme is given by [1:1:32, 48:16:448].

5. CONCLUSION

A novel non-uniform sampling pattern and reconstruction scheme was introduced to overcome the challenges associated with the iDQC MR spectroscopy scheme. The proposed scheme uses a non-uniform sampling scheme and a flexible partitioning of the spectral plane. The main objective was to reconstruct the metabolites with a good resolution and SNR, without being affected by aliases from the residual water region. Experimental data indicate that the non-uniform sampling pattern provides good reconstructions with narrow line-shapes, thus improving over the standard uniform reconstructions.

6. REFERENCES

[1] S W Provencher, "Estimation of metabolite concentrations from localized in vivo proton NMR spectra," *MRM*, vol. 30, no. 6, pp. 672–9, Dec 1993.

[2] Z Chen, Z Chen, and J Zhong, "High-resolution nmr spectra in inhomogeneous fields via ideal (intermolecular double quantum or single quantum coherences)," *J. Am. Chem. Soc*, Jan 2004.

[3] T Gu, Z Chen, X.Liu, L-C.Lin, and J.Zhong, "In vivo human whole cerebellum MRS under severe field inhomogeneity with iDQC method," in *ISMRM*, Nov 2008, Submitted.